PLOS ONE

RESEARCH ARTICLE

Conditional inference trees in the assessment of tree mortality rates in the transitional mixed forests of Atlantic Canada

Huiwen Guan[1,2], Xibin Dong[3]*, Guohua Yan[4], Tyler Searls[2], Charles P. -A. Bourque[2], Fan-Rui Meng[2]*

1 College of Economics & Management, Zhejiang University of Water Resources and Electric Power, Hangzhou, Zhejiang, China, **2** Faculty of Forestry and Environmental Management, University of New Brunswick, Fredericton, New Brunswick, Canada, **3** College of Engineering and Technology, Northeast Forestry University, Harbin, Heilongjiang, China, **4** Department of Mathematics and Statistics, University of New Brunswick, Fredericton, New Brunswick, Canada

* fmeng@unb.ca (FRM); xibindong@nefu.edu.cn (XD)

Citation: Guan H, Dong X, Yan G, Searls T, Bourque CP-A, Meng F-R (2021) Conditional inference trees in the assessment of tree mortality rates in the transitional mixed forests of Atlantic Canada. PLoS ONE 16(6): e0250991. https://doi.org/10.1371/journal.pone.0250991

Editor: Michal Bosela, Technical University in Zvolen, SLOVAKIA

Received: September 1, 2020

Accepted: April 16, 2021

Published: June 18, 2021

Data Availability Statement: The permanent sample plot and climatic datasets used in our study are owned by third-party organizations and were provided to us for use in this study under research agreements which contain clauses that prevent re-distribution of the data. For researchers who like to access the data, contact: New Brunswick Department of Natural Resources and Energy Development Hugh John Flemming Forestry Centre P. O. Box 6000 Fredericton, NB E3B 5H1 Canada (506) 453-3826 Fax: (506) 444-4367 Email: dnr_mrnweb@gnb.ca.

Abstract

Long-term predictions of forest dynamics, including forecasts of tree growth and mortality, are central to sustainable forest-management planning. Although often difficult to evaluate, tree mortality rates under different abiotic and biotic conditions are vital in defining the long-term dynamics of forest ecosystems. In this study, we have modeled tree mortality rates using conditional inference trees (CTREE) and multi-year permanent sample plot data sourced from an inventory with coverage of New Brunswick (NB), Canada. The final CTREE mortality model was based on four tree- and three stand-level terms together with two climatic terms. The correlation coefficient (R^2) between observed and predicted mortality rates was 0.67. High cumulative annual growing degree-days (GDD) was found to lead to increased mortality in 18 tree species, including *Betula papyrifera*, *Picea mariana*, *Acer saccharum*, and *Larix laricina*. In another ten species, including *Abies balsamea*, *Tsuga canadensis*, *Fraxinus americana*, and *Fagus grandifolia*, mortality rates tended to be higher in areas with high incident solar radiation. High amounts of precipitation in NB's humid maritime climate were also found to contribute to heightened tree mortality. The relationship between high GDD, solar radiation, and high mortality rates was particularly strong when precipitation was also low. This would suggest that although excessive soil water can contribute to heightened tree mortality by reducing the supply of air to the roots, occasional drought in NB can also contribute to increased mortality events. These results would have significant implications when considered alongside regional climate projections which generally entail both components of warming and increased precipitation.

Introduction

Long-term predictions of forest dynamics, including growth and species composition, are central to making sustainable forest-management decisions [1, 2]. Estimations of tree mortality

Funding: This research was funded in part by the China National Key Research and Development Program, grant number 2017YFC0504103, and by the New Brunswick Environmental Trust Fund. The funders had no role in study design, data collection and analysis, decision to publish, or preparation of the manuscript.

Competing interests: The authors have declared that no competing interests exist.

rates are particularly important in developing long-term predictions of forest dynamics as mortality not only influences total growing stock, but also affects stand structure [3], floristic composition [3], as well as nutrient and carbon cycling [4]. Despite their importance, reliable estimations of tree mortality rates under different biotic and abiotic site conditions are often difficult to obtain. This is because tree mortality is one of the least understood processes in forest ecosystems due to the complex, multi-scale interactions between growing-environment variables, as well as the influence of biotic and abiotic site factors [5]. Studies have attempted to establish connections between mortality and external factors, such as fire [6, 7], insect defoliation [8], and climatic variability [9, 10], but attempts to quantify internal sources of tree mortality are limited. These internal factors, including species identity [10], diameter at breast height [11], basal area [12], tree and stand age [13, 14], diameter growth rate [15], and stand competition [16–20] are known to each influence a tree's likelihood of mortality, although to what degree is frequently unclear.

Many models have been developed to estimate tree mortality probability distributions in accordance with tree, stand, and environmental factors [15]. Logistic regression is broadly used to model tree mortality rates and their inverse functions, tree survival rates [6, 15, 21–23]. The Kaplan-Meier method, which is a non-parametric method [10], as well as artificial intelligence have both been used to model tree mortality [24]. However, the transformation of modeled results from a probability distribution to meaningful tree mortality rates is seldom straightforward. Further still, most results tend to focus on tree-level, binary predictions of "dead or alive"; distributed randomly with a variance that is in accordance with tree characteristics [25]. Such predictions are most suitable for more simplistic stand structures [25, 26]. Where mixed forests are concerned, the representation provided by these methods becomes overly complex [6, 27]. The development of alternative methods to estimate tree mortality rates is, as a result, an active and much needed research area in forestry.

Classification and regression trees (CART) are an implementation of recursive partitioning, which has been applied across a diversity of fields, including data mining, wastewater treatment studies, and estimating landslide susceptibility [28–31]. Tree-structured models have the advantage that modeled results can be visually interpretable in the assessment of tree mortality rates. However, CART is susceptible to overfitting and selection biases, which favors covariates with more potential splits [28]. Conditional inference trees (CTREE) resolve the overfitting and selection bias problems associated with CART by applying suitable statistical tests to variable selection strategies and split-stopping criterion [32, 33]. The CTREE method has been employed in various contexts, such as in the testing of automobile engines [34] and in the characterization of myocardial infarctions [35, 36].

In this study, we use CTREE to model tree mortality rates for major commercial tree species in New Brunswick, Canada, using long-term tree data sourced from the provincial permanent sample plot (PSP) inventory [37]. We have also analyzed the impacts of environmental factors on tree mortality rates by species, giving particular attention to the influence of climatic variables, including precipitation and temperature.

Materials and methods

Study area

The study area for this research is the province of New Brunswick (NB), Canada (Fig 1). Forested area makes up more than 85% of the NB's seven million hectares (ha). The province is comprised of seven distinct ecoregions [38] (Table 1, Fig 1), classified based on prevalent climatic, geologic, topographic, and floristic communities and conditions [39]. NB's climate has characteristic cold, snowy winters, and warm, humid summers with an annual average

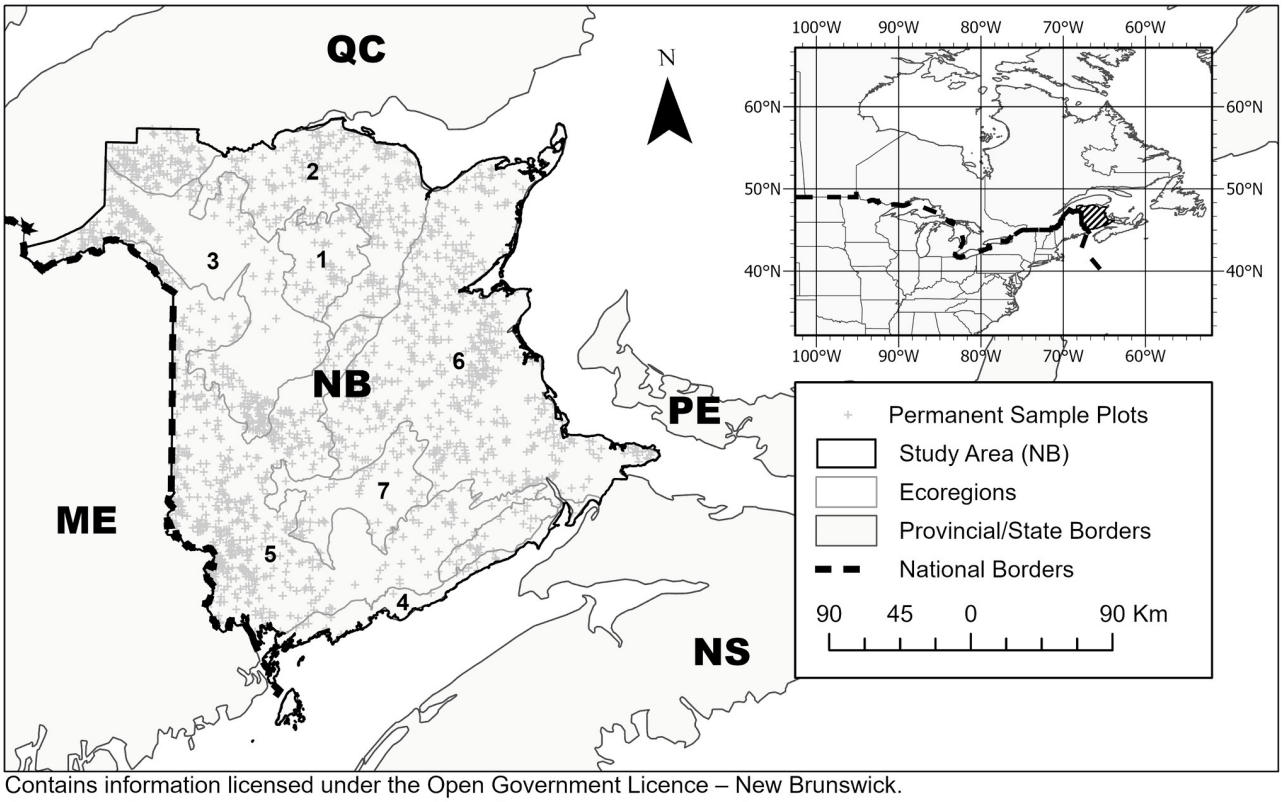

Fig 1. Location of permanent sample plots and ecoregions in New Brunswick of eastern Canada (inset). Ecoregion number in the legend corresponds to that in Table 1.

https://doi.org/10.1371/journal.pone.0250991.g001

temperature range from 2.0–6.3˚C. Mean annual precipitation ranges from 1,000–1,500 mm, with about half occurring as snow [40].

New Brunswick is home to 39 native tree species, the majority of which are conifers. Of these native species, 28 occur within the provinces permanent sample plot (PSP) inventory (Table 2). Commercially significant conifers include balsam fir (*Abies balsamea*), red spruce (*Picea rubens*), white spruce (*Picea glauca*), and black spruce (*Picea mariana*). Abundant shade

Table 1. Ecoregion and permanent sample plot (PSP) inventory summary, where A_r is the ecoregion land area (km^2), A_{rp} the proportion of NB that makes up the ecoregion (%), C_r the number of PSPs within the ecoregion, and C_{rp} the proportion of plots which constitute NB's total PSP inventory within a specific ecoregion (%).

Ecoregion No.	Ecoregion	Area		Plots	
		A_r	A_{rp}	C_r	C_{rp}
1	Highlands	4,908	6.74	421	11.65
2	Northern Uplands	8,761	12.03	577	15.97
3	Central Uplands	12,008	16.49	527	14.59
4	Fundy Coastal	2,223	3.05	39	1.08
5	Valley Lowlands	20,278	27.85	903	24.99
6	Eastern Lowlands	20,856	28.64	1,047	28.98
7	Grand Lake Lowlands	3,779	5.19	99	2.74
	Total	**72,813**		**3,613**	

https://doi.org/10.1371/journal.pone.0250991.t001

Table 2. Tree species common and scientific names, where N is the number of tree mortality observations.

Common Name	Scientific Name	Code	N
American Mountain Ash	*Sorbus americana*	AA	305
Black Ash	*Fraxinus nigra*	AB	607
White Ash	*Fraxinus americana*	AW	1,294
Grey Birch	*Betula populifolia*	BG	3,751
White Birch	*Betula papyrifera*	BW	33,489
Yellow Birch	*Betula alleghaniensis*	BY	13,040
Pin Cherry	*Prunus pensylvanica*	CP	1,950
Eastern White Cedar	*Thuja occidentalis*	EC	16,816
American Beech	*Fagus grandifolia*	EE	15,874
Eastern Hemlock	*Tsuga canadensis*	EH	1,418
Balsam Fir	*Abies balsamea*	FB	163,119
Hoptree	*Ptelea trifoliata*	IW	878
Speckled Alder	*Alnus incana*	KA	436
Tamarack	*Larix laricina*	LT	3,739
Mountain Maple	*Acer spicatum*	MM	1,868
Red Maple	*Acer rubrum*	MR	56,676
Sugar Maple	*Acer saccharum*	MS	24,358
Striped Maple	*Acer pensylvanicum*	MT	5,436
Red Oak	*Quercus rubra*	OR	267
Jack Pine	*Pinus banksiana*	PJ	8,142
Red Pine	*Pinus resinosa*	PR	448
Balsam Poplar	*Populus balsamifera*	RB	776
Large-tooth Aspen	*Populus grandidentata*	RL	1,561
Trembling Aspen	*Populus tremuloides*	RT	21,137
Black Spruce	*Picea mariana*	SB	108,378
Red Spruce	*Picea rubens*	SR	62,614
White Spruce	*Picea glauca*	SW	21,158
Willow	*Salix nigra*	XW	257

https://doi.org/10.1371/journal.pone.0250991.t002

intolerant hardwoods include trembling aspen (*Populus tremuloides*), red maple (*Acer rubrum*), and white birch (*Betula papyrifera*), whereas shade tolerant hardwoods include yellow birch (*Betula alleghaniensis*), sugar maple (*Acer saccharum*), ironwood (*Ostrya virginiana*), black cherry (*Prunus serotina*), white ash (*Fraxinus americana*), red oak (*Quercus sp.*), and American beech (*Fagus grandifolia*) [41].

Permanent sample plot data

NB's permanent sample plot (PSP) inventory is maintained by the NB Department of Energy and Resources Development. The network containing nearly 1,900 PSPs, more than 165,000 individual trees, and 580,000 tree measurements spanning a period from 1985–2014 [37]. Plots in NB use a standard area of 400 m^2 and are re-measured at periods of 3 or 5 years depending on stand age [37]. The spatial distribution of NB's network of PSPs is illustrated in Fig 1. Tree species and diameter at breast height (DBH) are recorded by technicians for every live tree in the plot with a DBH $>$ 5.1 cm. All tree records from PSPs that had been subject to fire, insect defoliation, windthrow, or timber harvesting were excluded from the analysis. The modeling methods employed cannot account for the stochastic nature of large-scale mortality (or 'calamity') events.

Table 3. Listing of independent variables for tree rate of mortality modeling.

Variable	Explanation	Class
ΔBA	Average annual basal area growth increment between two plot measurements ($cm^2\ yr^{-1}$)	Tree-level
SP	Species	Tree-level
AGE	Age class	Tree-level
BAL	Total basal area of all trees with diameter > diameter of the subject tree ($m^2\ ha^{-1}$)	Tree-level
GDD	Growing degree-days (degree-day units)	Climatic
PCP	Precipitation (mm)	Climatic
INS	Potential solar radiation ($Wh\ m^{-2}$)	Stand-level
SLP	Slope (%)	Stand-level
ERD	Relative density (%)	Stand-level

https://doi.org/10.1371/journal.pone.0250991.t003

In NB's PSP inventory, tree age is estimated within plots using the measured age of sample trees located immediately outside plots; this minimizes the potential of injuring trees within the plot through the increment coring process. Sample tree age is then used to inform age class (es) present within a plot. All stems within the plot are then assigned an age class by technicians undertaking plot measurements. Age is only measured once within a plot's lifecycle; observed as part of the plot establishment record. A collection of approximately 27,500 sample age measurements informs all tree age measurements in NB's PSP inventory.

Model development

Data quality control and variable selection. A complete list of independent variables is provided in Table 3. Tree species were coded as a nominal variable, with 28 species levels (Table 2).

Tree-level variables. Tree age is often used as the basis for models of individual-tree rate of mortality [23, 42–44]. In this study, four age classes were used as independent levels constituting the nominal AGE covariate: young, immature, mature, and overmature. Tree growth rates are also commonly used to estimate the probability of tree survival [5, 45]. In this study, the average annual basal area growth increment for individual trees (ΔBA), as measured between two consecutive BA measurements, was also selected as an independent variable:

$$\Delta BA_i = \frac{BA_i - BA_{i-1}}{t_i - t_{i-1}} \quad (1)$$

where BA_i is the tree basal area at the i^{th} measurement, and t_i is the corresponding year of measurement. Observations of $\Delta BA > 0.02$ cm yr^{-1} were considered outliers and were removed from the study.

Competition. Trees in stands face competitive interactions [20, 46, 47]. We used two variables to capture the influence of competition on tree mortality, namely (i) the total basal area of stands for trees thicker than the subject tree (BAL_i), and (ii) an extended relative density index (ERD). The BAL_i index reflects the relative advantage of the tree as compared to other trees in the plot, and was calculated as the sum of total basal area of all trees with DBH's greater than that of the subject tree [23, 48], i.e.,

$$BAL_i = \left(\sum_{j=1}^{m} BA_j\right)\left(\frac{10000}{AP}\right) \quad (2)$$

where BAL_i is the total basal area of trees greater than i^{th} tree (m^2), AP the size area of the PSP (m^2), BA_j the basal area of the j^{th} tree, and m the number of trees in the plot with DBH greater

or equal to the DBH of the i^{th} tree. *ERD* was developed in this study as a ratio between stand density and the maximum potential density of the stand to further account for overall competition intensity within the stand. The maximum potential density of the stand was calculated based on the law of self-thinning [46]. In accordance with the law, the maximum number of trees a stand can support decreases exponentially with mean tree size, i.e.,

$$N_{max} = \alpha\left(\frac{DBH}{DBH_r}\right)^{-\beta} \quad (3)$$

where N_{max} is the maximum potential density of the stand with mean DBH. Parameter α is the maximum density at an arbitrary reference DBH_r (set at 20 cm for this study, [68, 69]), and β is a self-thinning coefficient. In this study, we assume N_{max} to be constant irrespective of stand composition and age. For a stand with density N (stems ha^{-1}), the extended relative density is then giving as,

$$ERD = \frac{N}{N_{max}} = \frac{n}{\alpha}\left(\frac{DBH}{DBH_r}\right)^{\beta} \quad (4)$$

Because *ERD* and *BAL* are closely related, but represent different aspects of competition-induced tree mortality, one interaction covariate, *BAL*×*ERD* was used to accommodate competitive forces in the CTREE model. Observations of $BAL \times ERD > 7$ were considered outliers and were removed from further consideration.

Stand-level climatic factors. Four stand-level climatic (i.e., abiotic) factors were included in the analysis, i.e., annual precipitation (PCP), potential solar radiation (INS), annual cumulative growing degree-days (GDD), and slope. Slope was included here as a stand-level factor, as it was anticipated to be a fair proxy of soil moisture conditions within a given PSP. Fine-scale soils information, such as depth, porosity, and frost-depths were unavailable for the study area. A percentage slope surface was calculated from a digital elevation model (DEM) interpolated at 1-m resolution [49]. Plot slope was then estimated as the average slope within a 40-m radius from the plot center. Plots where slope observations > 40% were considered outliers and were removed from the study. Potential solar radiation was calculated as the sum of direct and diffuse solar radiation. DEM-based INS was determined as a function of solar angle by latitude, slope, as well as aspect, and was evaluated as a raster surface [50]. As with the slope variable, plot estimations of INS (in Wh m^{-2}) were calculated as the average within a 40-m radius from the plot center.

Utilizing the same methods leveraged in the JABOWA-family of forest gap models, GDD was estimated using only monthly mean daily temperatures [51]. In the estimation of GDD, the base temperature below which tree growth is assumed to be negligible [51] was assumed to be 4.4˚C for all species. Monthly mean daily temperatures at each PSP were determined through monthly mean daily maximum and minimum temperatures, as generated with ANUSPLIN, a non-parametric surface-fitting procedure [52]. The ANUSPLIN-generated datasets used herein were based on records obtained from weather stations and then interpolated over topographic surfaces. Through the same approach we also obtained estimates of cumulative monthly PCP, which we then used to determine cumulative annual PCP. The historical monthly models generated with ANUSPLIN have 95% confidence limits of approximately ±1.1 and ±1.3˚C for maximum and minimum daily temperatures, respectively, and 10–40% for monthly PCP [52]. Both cumulative annual PCP and GDD were employed as the annual average between previous and current subject measurements.

A five-year tree rate of mortality during the period between two consecutive measurements served as the only dependent variable. Rate of mortality was estimated based on tracking

individual trees over time and taking note of their mortality-status change. As a general practice, tree status was coded as "alive" or "dead" at the time of inventory measurement. In this study, living trees were coded as 1, and dead trees as 0. Repeated codes of 0 for the same tree were deleted following the earliest instance of code 0. This avoided repeated counting of dead trees. To calculate rate of mortality, all data were divided into groups according to species and other independent variables (Table 2), with an objective to minimize the within-group mortality rates. Those groups with insufficient records (< 20) were eliminated. After that, the five-year mortality rates were calculated based on the number of dead trees during the measurement period in the group and the total number of living trees at the beginning of the measurement period. For a remeasurement period of other than five years, the method introduced by Flewelling and Monserud [70] was used to convert 3-year mortality rates (P_{m3}) to five-year rates by means of $P_{m5} = 1-(1-P_{m3})^{5/3}$.

Covariate testing

To test for multicollinearity, a correlation matrix was prepared using each of the nine covariates (Fig 2). Spearman rank correlation was used to determine correlation values [53].

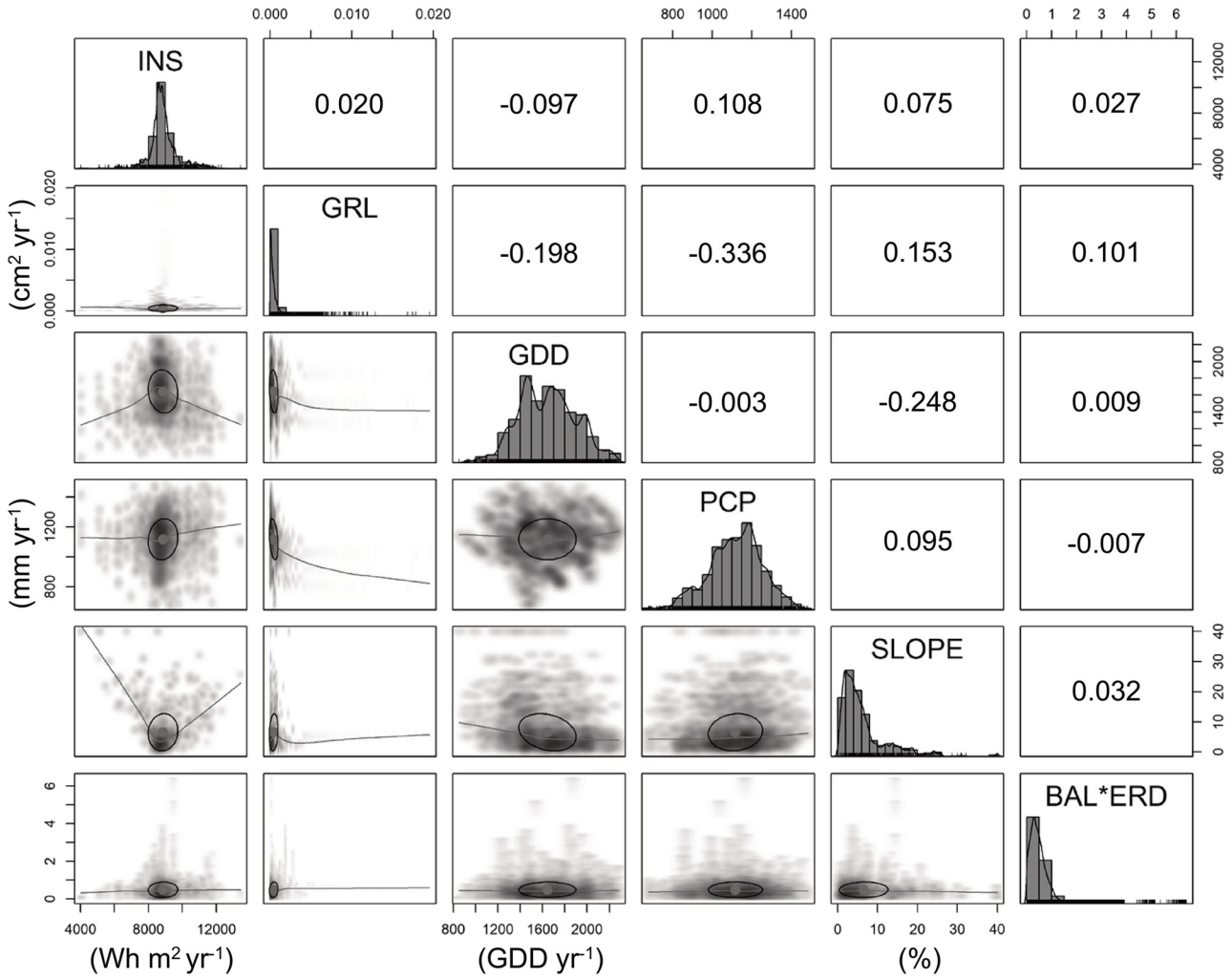

Fig 2. Correlation matrix for the nine independent variables used in the modeling methods. Variable distribution is shown along the diagonal, Spearman rank correlation between the corresponding independent variables in the upper right quadrant.

https://doi.org/10.1371/journal.pone.0250991.g002

Commonly, Spearman correlation coefficients between 0.10 and 0.29 represent a slight association, those between 0.30 and 0.49 represent some association, and those > 0.50 represent a significant association or relationship. We found most independent variables to have no correlation with one and other (Fig 2). Potential solar radiation (INS), however, correlated slightly with precipitation (PCP), as did growth increment (ΔBA) with $BAL{\times}ERD$; ΔBA was also found to correlate slightly with slope (SLP). Correlation amongst model covariates was determined to not be of significant concern.

Model structure

The CTREE mortality model was fitted using the "*partykit*" package in R [36, 54]. CTREE generates a nonlinear mortality diagram, which gives a tree-shape probability map of tree mortality rates. The initial bifurcation was determined through multiplicity-adjusted p-values, in accordance with Bonferroni's criterion [36, 54]. CTREE is implemented through the following protocol [36, 54], i.e., at each stage, CTREE determines the optimal split of a region in the feature space assembled by variables that affect tree mortality and partitioned according to the Bonferroni criterion [36]. The splitting process starts by using the entire feature space and repeats, informing successive splits using the remaining feature space. This process continues with risk-tree development and pruning until the terminal node is realized and no subsequent splits are possible. The probability of a tree dying is calculated at each terminal node, which yields a stratified model.

Model evaluation and comparison

Correlation coefficients between observed measurements and model predictions, as well as mean square error (MSE) and mean biases were used to assess the model. Furthermore, cross validation of CTREE model was completed through a k-fold test [55]. The original dataset was randomly partitioned into 5 subsamples (k = 5). One subsample (20% of the data in the original dataset) was chosen to serve as the test series for cross validation, and the remaining four subsamples (20% each) for model development (training). The cross-validation process was repeated 5 times, with each subsample being utilized once for training purposes. A two-tailed p-value < 0.05 was considered statistically significant.

Results and discussion

The correlation coefficient between observed and predicted mortality was 0.67, with a MSE of 0.006. Mean bias was observed to be < 0.001. The final mortality model had 56 inner nodes and 57 terminal nodes (Figs 3 and 4). For purposes of discussion, notation N36 refers to Node 36, N47 to Node 47, and so forth.

Through the k-fold test, correlation coefficients ranged from 0.59 to 0.62 with a mean of 0.61, and MSE ranged from 0.006 to 0.008, with mean of 0.007. The difference in correlation coefficients between each k-fold subset was < 0.03, suggesting that the accuracy of the CTREE procedure to be relatively stable, even with a reduced sample size. CTREE's branching structure was affected by the reduced sample size used in the k-fold validation, i.e., the number of terminal nodes in the k-fold mortality models ranged from 43 to 52, and the number of inner nodes from 42 to 51. We observed that despite these structural differences, the higher-order splits from 1 to 4 of the CTREE did not change between k-fold subsets (Figs 3 and 4). Rather, most differences in split structure were found to occur amongst the lower branches of the probability tree. The split in Node 28 (the one associated with PCP) was not common to all data subsets. One instance was found to appear after the species split. Precipitation (PCP) was an important contributor to tree mortality in both probability tree structures, but the

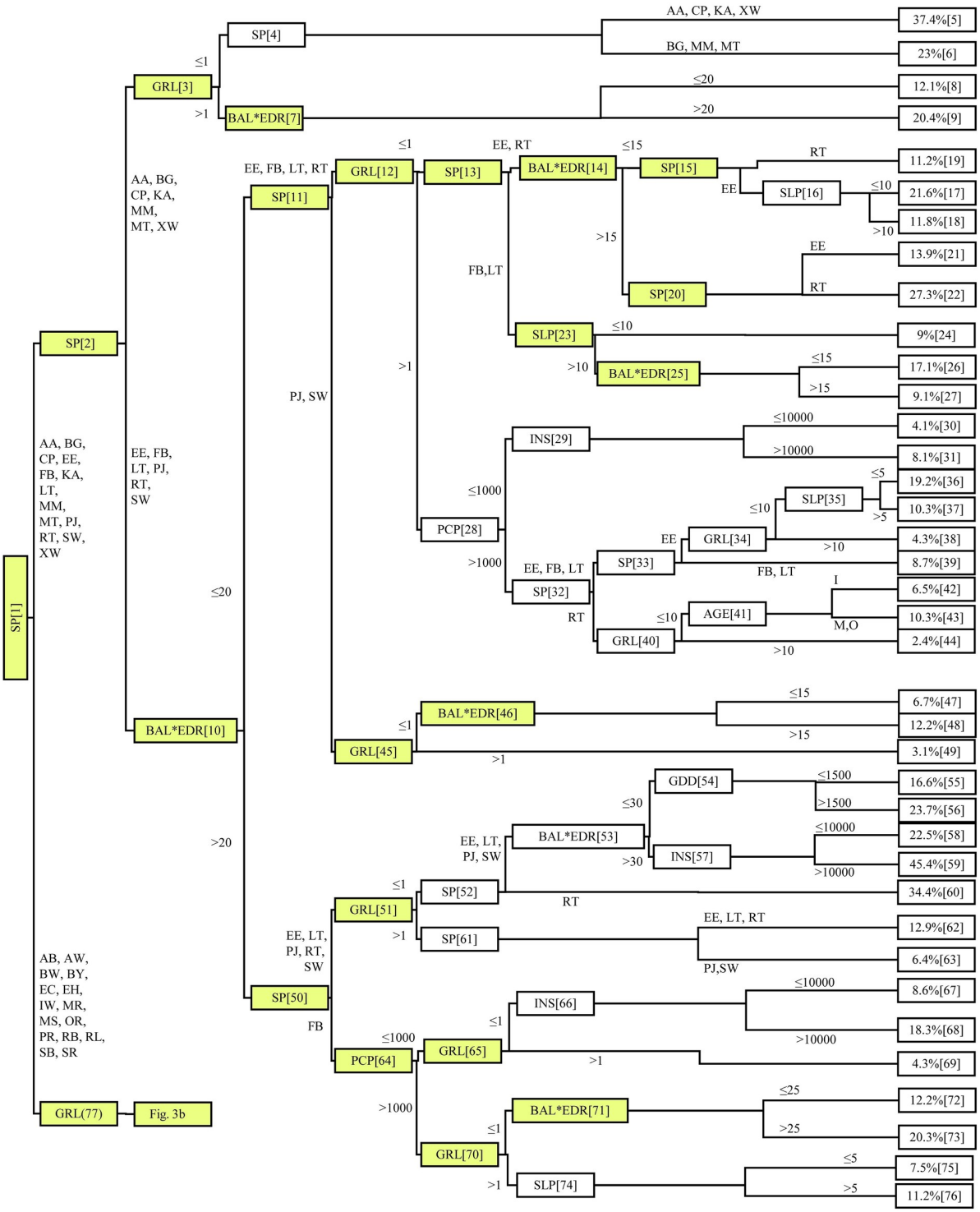

Fig 3. Nodes 1–76 of the conditional inference tree (CTREE) of rate of mortality for 28 boreal and temperate species (see Table 2, for code definition). Tree-level variables include species (SP), average annual basal area growth increment (*ΔBA*), basal area of the largest tree and relative density interaction (*BAL*×*EDR*). Stand-level variables include potential solar radiation (INS) and slope (SLP). Climatic variables include cumulative annual growing degree-days (GDD) and cumulative annual precipitation (PCP). The terminal nodes, 38 in total, show the proportion of dead trees. Nodes shaded yellow were consistent in all folds in model cross-validation.

https://doi.org/10.1371/journal.pone.0250991.g003

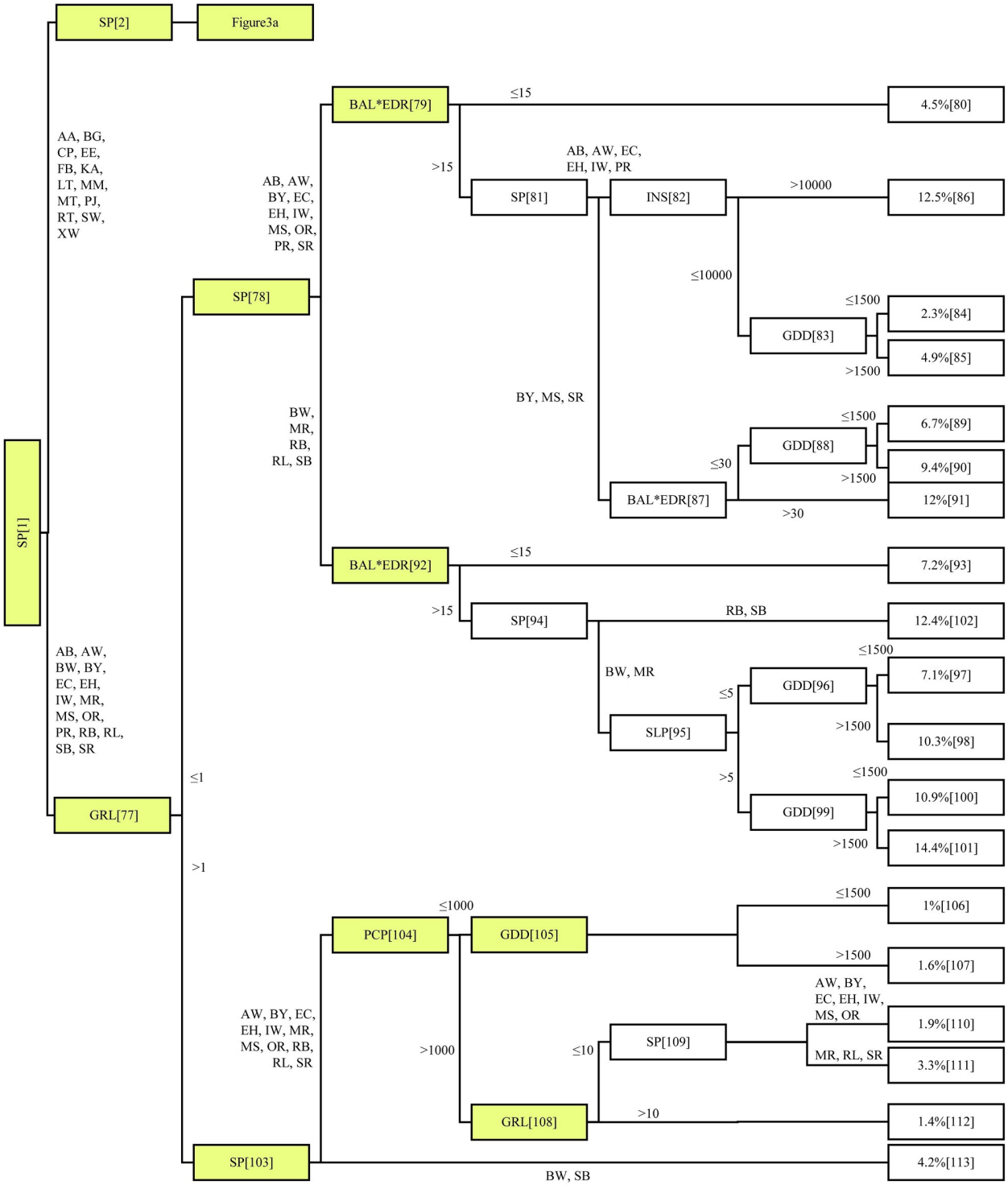

Fig 4. Nodes 77–108 of the conditional inference tree (CTREE) of rate of mortality for 28 boreal and temperate species (see Table 2, for code definition). Tree-level variables include species (SP), average annual basal area growth increment (*ΔBA*), basal area of the largest tree and relative density interaction (*BAL×EDR*). Stand-level variables include potential solar radiation (INS), and slope (SLP). Climatic variables include cumulative annual growing degree days (GDD) and cumulative annual precipitation (PCP). The terminal nodes, 19 in total, show the proportion of dead trees. Nodes shaded yellow were consistent in all folds in model cross-validation.

https://doi.org/10.1371/journal.pone.0250991.g004

relationship to other covariates markedly differed. Such an observation confirms the significance of sample size in the fit of the probability tree. In more than one of the CTREE-models prepared as part of the k-fold testing, the splits at N4 and N7 were not present (Fig 3). This result identifies that the CTREE method can avoid issues of overfitting by eliminating frivolous nodes where the input dataset does not support additional branching before the terminal node. The CTREE method offers a mortality modeling approach where complex nonlinear relationships between covariates and mortality rates are determined through the CTREE model package. This is in contrast to many established mortality modeling approaches, where the nonlinear relationships between covariates and mortality rates depend on having a prior understanding and stipulating through model development [56, 57]. Frequently, the empirical study of such nonlinear relationships between variables in the growing environment and tree mortality is not available.

Influence of tree-level variables on tree mortality

We found that the species covariate SP was the most important discriminator, appearing not only for the first split, but for subsequent splits as well (Figs 3 and 4). Red oak and eastern hemlock have the lowest rate of mortality range between 1.00–1.90% (N105, N108, and N109; Fig 4). Balsam fir was found to have significant variability in rate of mortality, ranging from 8.80% (N33) to 20.3% (N71; Fig 3). The high variability in balsam fir mortality rate is intuitive, given the species is short-lived and has a tendency to form high-density cover [58], whereas oak and hemlock are long-lived, shade tolerant hardwoods [59]. Annual growth rate was found to be the most important predictor of tree mortality [5, 45]. Studies have previously found tree mortality and growth to be inversely related [60, 61], and furthermore, that tree growth is continuous through life in uneven aged stands [62]. Low ΔBA was also found to lead to higher mortality rates (Fig 2a). Mortality was as high as 23–37.4% (moderated by species) whenever $\Delta BA \leq 1$ cm^2 5-yr^{-1}, as compared to 12.1–20.4% (moderated by competition indices) when $\Delta BA > 1$ cm^2 5-yr^{-1} (Fig 3). Similar results were observed through N12, N45, N51, N65, N70, and N77 (Figs 3 and 4). When $\Delta BA > 10$ cm^2 5-yr^{-1}, rate of mortality was generally reduced, e.g., a rate of mortality of 2.4% was observed when $\Delta BA > 10$ cm^2 5-yr^{-1}, but 8.4% when $\Delta BA \leq 10$ cm^2 5-yr^{-1} (i.e., N40; Fig 3).

The AGE covariate appeared only once in the CTREE mapping (i.e., N41; Fig 3); branching trembling aspen mortality rates. Aspen mortality rates were 6.5% and 10.3% for immature trees and mature/overmature trees, respectively. This split only occurred where aspen $\Delta BA <$ 10 cm^2 5-yr^{-1} through the preceding five years. When $\Delta BA > 10$ cm^2 5-yr^{-1}, aspen mortality rate was 2.4%, regardless of AGE class. Perhaps contrary to intuition, our results do not support age effects as a significant contributor to rate of mortality. This could be attributed to two causalities, (i) the forests in the study area are intensively managed with few trees reaching full maturity and succumbing to age-related mortality, and (ii) given the inclusion of ΔBA as an independent variable, age effects may be indirectly applied through that term, as overmature trees tend to stop growing before mortality occurs. Still, the correlation matrix (Fig 2) identified no collinearity between ΔBA and AGE.

Influence of competition on tree mortality

The impacts of *BAL* appear to be absorbed by the interaction between *BAL* and *EDR*, i.e., greater interaction-values associated with higher mortality rates. As shown in Fig 3, through N10, the average rate of mortality was 10.85% when $BAL \times EDR \leq 20$, as compared to 17.52 when $BAL \times EDR > 20$ (*BAL* in cm^2 and *EDR* in number of stems per ha). Similar results were observed with CTREE N14, N25, N46, N79, N53, N87, and N92 (Figs 3 and 4). Variables

representing competitive interactions were associated with higher mortality rates. As the two variables were used to reflect different competitive concerns, we found an interaction term to offer the best means to include the two otherwise intimately related parameters. Due to the generalized significance of this interaction to tree mortality, we can conclude that competition is one of the important factors causing death in trees. Indeed, studies have found that the majority of trees die young due to competitive pressures [63]. Other studies have found mortality rates to increase with increased water deficits and stand basal area [64].

Influence of climate and site conditions on tree mortality

We found PCP to appear three times in N28, N64, and N104, and again in N35, N74, and N95 for SLP (Figs 3 and 4). High tree mortality rates were often coincidental with PCP $<$ 1000 mm yr^{-1} (Figs 3 and 4). Through N28 (Fig 3), mortality rates for American beech, balsam fir, tamarack, and trembling aspen were 4.1–8.1% when PCP was $<$ 1000 mm yr^{-1}, and 2.4–19.2% when $>$ 1000 mm yr^{-1}. The mean slope (SLP) appeared to have a synergistic relationship with PCP, as observed in N35, where the rate of mortality for American beech was 19.2% when PCP $>$ 1000 mm yr^{-1} and SLP $<$ 5%, as compared to 10.3% when SLP $>$ 5%. Still, SLP $<$ 5% was not always associated with lower rate of mortality. Through N99 (Fig 4), SLP $<$ 5% was associated with a lower white birch and red maple mortality rate (7.1–10.3%) as compared to 10.9–14.4% when SLP was $>$ 5%. A similar trend was observed for balsam fir (N74), with a mortality rate of 7.5% with SLP $>$ 5%, compared to 11.2% with SLP $<$ 5%. In general, the impact of PCP and SLP were species dependent, and often synergistic with other independent terms in the CTREE model.

Solar radiation (INS) was found to increase the rate of mortality in four CTREE splits (N29, N57, N66 and N82; Figs 3 and 4). Through N29, mortality rates in four tree species (i.e., American beech, balsam fir, tamarack, and trembling aspen) were 4.1% when INS $\leq$ 10000 Wh m^{-2} and 8.1% when INS $>$ 10000 Wh m^{-2}. As INS has a warming effect on microclimate, in addition to direct impacts on photosynthetic potential, there may have been some overlap between GDD and INS. In this study, INS did not consider the year-to-year variations in cloud cover and associated reductions in available sunlight. Furthermore, our correlation matrix did not identify significant collinearity between the independent terms (Fig 2). We found the relationship between GDD and tree mortality to be mixed, splitting at six locations (N54, N83, N88, N96, N99, and N105), and involving 18 special interactions (Figs 3 and 4). In all cases, GDD $>$ 1500 was associated with increased rate of mortality. Through N96, as an example, rate of mortality for white birch and red maple was 7.1% at $<$ 1500 and 10.3% at $>$ 1500 degree-days. Essentially, this characterization would suggest that a mean increase in regional temperatures, as is often attributed to changing climate, could lead to greater mortality in some tree species in NB.

PCP $<$ 1000 mm yr^{-1} and GDD $>$ 1500, possibly indicative of localized drought, contributed to a high rate of mortality (N106 *vs*. N107; Fig 4). This indicates that although excessive soil water content can lead to high mortality rates (i.e., SLP $<$ 5%, PCP $>$ 1000 mm yr^{-1}, N36; Fig 3), occasional drought can also lead to high tree mortality rates, in agreement with other researchers' findings [65]. For example, Peng et al. [65] found that drought conditions can induce an increase in tree mortality rate in old-growth forests. In general, our results identify that climatic variables, including GDD, cumulative annual PCP, and INS had significant impact on tree mortality rates for some tree species. There is a wealth of scientific literature that support the significance of climate to tree growth [9, 66, 67].

CTREE offers a viable method for estimating mortality rates in mixedwood, boreal-temperate ecotone making up the New England-Acadian forest. This study included nine

independent variables within the CTREE model, none of which have been determined to be significantly collinear with one and another (Fig 2). Through the design phases of this study program, we undertook various tests to explore the value of an array of potential covariates, eliminating those which did not offer a significant contribution to the final mortality model. While we recognize that certain covariates may have a lesser influence on tree mortality rate (e.g., *BAL*×*EDR* and INS), the inclusion of these terms improved the overall explanatory power of the model in our analysis. If either term (i.e., *BAL*×*EDR* and INS) was removed from the final CTREE model, the correlation coefficients would have been reduced from 0.671 to 0.597 or to 0.659, respectively. The decision to include the nine variables we ultimately chose was governed in large part by the breadth of the datasets available. While we recognize that tree mortality is an incredibly complex process, which is influenced by an exhaustive array of forest variables and interactions, the modeling methods employed in this study do not attempt to illuminate the influence of stochastic [68, 69] or periodic [70] disturbance on tree mortality rates. The influence of these type of disturbances on mortality would need to be considered alongside our CTREE model in any practical application of the methods.

Conclusions

Perhaps intuitively, our CTREE approach to mortality confirmed rate of tree growth and competitive interactions at the stand-level as important determinants of tree mortality rate. We found GDD and INS to increase mortality for 18 species, including white birch, black spruce, sugar maple, and tamarack. We also found that high PCP and shallow SLP commonly contributed to and increased tree mortality rates, presumably as a result of excess soil water in some parts of NB. We observed that low PCP in combination with high GDD or high INS often led to elevated tree mortality, potentially indicative of the effects of drought. These observations may have significant implications when considered alongside regional climate projections for NB, which generally entail both components of warming and increased precipitation. The major contribution offered by the CTREE approach is the expanded capacity to reveal complex nonlinear relationships in mortality, without the relationships needing to be known *a priori*, as is commonly the case in tree mortality modeling. There is potential that the CTREE method may offer an improved means to modeling tree mortality in complex forested ecosystems, such as the New England-Acadian forest ecotone. In addition, the CTREE model could be directly integrated with forest growth and yield models, further bolstering the approach's operational potential.

Acknowledgments

We would like to thank the Forest Growth and Yield Group of New Brunswick Department of Natural Resources and Energy Development for the provision of their forest inventory data, and the Canadian Forest Service for the provision of their reconstructed weather record data.

Author Contributions

Conceptualization: Xibin Dong, Guohua Yan, Fan-Rui Meng.

Data curation: Tyler Searls, Charles P. -A. Bourque, Fan-Rui Meng.

Formal analysis: Huiwen Guan, Guohua Yan, Fan-Rui Meng.

Funding acquisition: Xibin Dong, Fan-Rui Meng.

Investigation: Xibin Dong, Tyler Searls, Fan-Rui Meng.

Methodology: Fan-Rui Meng.

Project administration: Xibin Dong.

Resources: Fan-Rui Meng.

Supervision: Xibin Dong, Charles P. -A. Bourque, Fan-Rui Meng.

Validation: Guohua Yan.

Visualization: Fan-Rui Meng.

Writing – original draft: Huiwen Guan, Charles P. -A. Bourque, Fan-Rui Meng.

Writing – review & editing: Huiwen Guan, Xibin Dong, Guohua Yan, Tyler Searls, Charles P. -A. Bourque, Fan-Rui Meng.

References

1. Chapman RA, Heitzman E, Shelton MG. Long-term changes in forest structure and species composition of an upland oak forest in Arkansas. Forest Ecology and Management, Vol 236: 85–92. 2006 [cited 30 Jul 2020]. https://www.fs.usda.gov/treesearch/pubs/24967
2. Soares P, Tomé M, Skovsgaard JP, Vanclay JK. Evaluating a growth model for forest management using continuous forest inventory data. Forest Ecology and Management. 1995; 71: 251–265. https://doi.org/10.1016/0378-1127(94)06105-R
3. de Toledo JJ, Magnusson WE, Castilho CV. Competition, exogenous disturbances and senescence shape tree size distribution in tropical forest: evidence from tree mode of death in Central Amazonia. Journal of Vegetation Science. 2013; 24: 651–663. https://doi.org/10.1111/j.1654-1103.2012.01491.x
4. Fontes CG, Chambers JQ, Higuchi N. Revealing the causes and temporal distribution of tree mortality in Central Amazonia. Forest Ecology and Management. 2018; 424: 177–183. https://doi.org/10.1016/j.foreco.2018.05.002
5. Bigler C, Bugmann H. Predicting the Time of Tree Death Using Dendrochronological Data. Ecological Applications. 2004; 14: 902–914. https://doi.org/10.1890/03-5011
6. Botequim B, Arias-Rodil M, Garcia-Gonzalo J, Silva A, Marques S, Borges J, et al. Modeling Post-Fire Mortality in Pure and Mixed Forest Stands in Portugal—A Forest Planning-Oriented Model. Sustainability. 2017; 2017: 390. https://doi.org/10.3390/su9030390
7. Whittier TR, Gray AN. Tree mortality based fire severity classification for forest inventories: A Pacific Northwest national forests example. Forest Ecology and Management. 2016; 359: 199–209. https://doi.org/10.1016/j.foreco.2015.10.015
8. Jaime L, Batllori E, Margalef-Marrase J, Pérez Navarro MÁ, Lloret F. Scots pine (Pinus sylvestris L.) mortality is explained by the climatic suitability of both host tree and bark beetle populations. Forest Ecology and Management. 2019; 448: 119–129. https://doi.org/10.1016/j.foreco.2019.05.070
9. Allen CD, Macalady AK, Chenchouni H, Bachelet D, McDowell N, Vennetier M, et al. A global overview of drought and heat-induced tree mortality reveals emerging climate change risks for forests. Forest Ecology and Management. 2010; 259: 660–684. https://doi.org/10.1016/j.foreco.2009.09.001
10. Das AJ, Stephenson NL, Flint A, Das T, van Mantgem PJ. Climatic Correlates of Tree Mortality in Water- and Energy-Limited Forests. Bohrer G, editor. PLoS ONE. 2013; 8: e69917. https://doi.org/10.1371/journal.pone.0069917 PMID: 23936118
11. Hamilton DA. A Logistic Model of Mortality in Thinned and Unthinned Mixed Conifer Stands of Northern Idaho. for sci. 1986; 32: 989–1000. https://doi.org/10.1093/forestscience/32.4.989
12. Glover GR, Hool JN. A Basal Area Ratio Predictor of Loblolly Pine Plantation Mortality. for sci. 1979; 25: 275–282. https://doi.org/10.1093/forestscience/25.2.275
13. Hiroshima T. Applying age-based mortality analysis to a natural forest stand in Japan. Journal of Forest Research. 2014; 19: 379–387. https://doi.org/10.1007/s10310-013-0428-8
14. Larson AJ, Lutz JA, Donato DC, Freund JA, Swanson ME, HilleRisLambers J, et al. Spatial aspects of tree mortality strongly differ between young and old-growth forests. Ecology. 2015; 96: 2855–2861. https://doi.org/10.1890/15-0628.1 PMID: 27070005
15. Wyckoff PH, Clark JS. The relationship between growth and mortality for seven co-occurring tree species in the southern Appalachian Mountains. Journal of Ecology. 2002; 90: 604–615. https://doi.org/10.1046/j.1365-2745.2002.00691.x
16. Adams HD, Guardiola-Claramonte M, Barron-Gafford GA, Villegas JC, Breshears DD, Zou CB, et al. Temperature sensitivity of drought-induced tree mortality portends increased regional die-off under

global-change-type drought. PNAS. 2009; 106: 7063–7066. https://doi.org/10.1073/pnas.0901438106 PMID: 19365070

17. Breshears DD, Cobb NS, Rich PM, Price KP, Allen CD, Balice RG, et al. Regional vegetation die-off in response to global-change-type drought. PNAS. 2005; 102: 15144–15148. https://doi.org/10.1073/pnas.0505734102 PMID: 16217022
18. Lines ER, Coomes DA, Purves DW. Influences of Forest Structure, Climate and Species Composition on Tree Mortality across the Eastern US. PLOS ONE. 2010; 5: e13212. https://doi.org/10.1371/journal.pone.0013212 PMID: 20967250
19. Ruiz-Benito P, Lines ER, Gómez-Aparicio L, Zavala MA, Coomes DA. Patterns and Drivers of Tree Mortality in Iberian Forests: Climatic Effects Are Modified by Competition. PLOS ONE. 2013; 8: e56843. https://doi.org/10.1371/journal.pone.0056843 PMID: 23451096
20. Boeck A, Dieler J, Biber P, Pretzsch H, Ankerst DP. Predicting Tree Mortality for European Beech in Southern Germany Using Spatially Explicit Competition Indices. for sci. 2014; 60: 613–622. https://doi.org/10.5849/forsci.12-133
21. Preisler HK, Slaughter GW. A Stochastic Model for Tree Survival in Stands Affected by Annosum Root Disease. for sci. 1997; 43: 78–86. https://doi.org/10.1093/forestscience/43.1.78
22. Vanclay JK. Synthesis: Growth Models for Tropical Forests: A Synthesis of Models and Methods. for sci. 1995; 41: 7–42. https://doi.org/10.1093/forestscience/41.1.7
23. Monserud RA, Sterba H. Modeling individual tree mortality for Austrian forest species. Forest Ecology and Management. 1999; 113: 109–123. https://doi.org/10.1016/S0378-1127(98)00419-8
24. Reis LP, de Souza AL, dos Reis PCM, Mazzei L, Soares CPB, Miquelino Eleto Torres CM, et al. Estimation of mortality and survival of individual trees after harvesting wood using artificial neural networks in the amazon rain forest. Ecological Engineering. 2018; 112: 140–147. https://doi.org/10.1016/j.ecoleng.2017.12.014
25. Fajardo SN, Valenzuela S, Santos AFD, González MP, Sanfuentes EA. Phytophthora pseudosyringae associated with the mortality of Nothofagus obliqua in a pure stand in central-southern Chile. Forest Pathology. 2017; 47: e12361. https://doi.org/10.1111/efp.12361
26. Moulinier J, Lorenzetti F, Bergeron Y. Growth and mortality of trembling aspen (Populus tremuloides) in response to artificial defoliation. Acta Oecologica. 2014; 55: 104–112. https://doi.org/10.1016/j.actao.2013.12.007
27. Manso R, Morneau F, Ningre F, Fortin M. Incorporating stochasticity from extreme climatic events and multi-species competition relationships into single-tree mortality models. Forest Ecology and Management. 2015; 354: 243–253. https://doi.org/10.1016/j.foreco.2015.06.008
28. Breiman L, Friedman J, Stone CJ, Olshen RA. Classification and Regression Trees. 1 edition. Boca Raton: Chapman and Hall/CRC; 1984.
29. Chrysos G, Dagritzikos P, Papaefstathiou I, Dollas A. HC-CART: A parallel system implementation of data mining classification and regression tree (CART) algorithm on a multi-FPGA system. ACM Trans Archit Code Optim. 2013; 9: 47:1–47:25. https://doi.org/10.1145/2400682.2400706
30. Suchetana B, Rajagopalan B, Silverstein J. Assessment of wastewater treatment facility compliance with decreasing ammonia discharge limits using a regression tree model. Science of The Total Environment. 2017; 598: 249–257. https://doi.org/10.1016/j.scitotenv.2017.03.236 PMID: 28441603
31. Youssef AM, Pourghasemi HR, Pourtaghi ZS, Al-Katheeri MM. Landslide susceptibility mapping using random forest, boosted regression tree, classification and regression tree, and general linear models and comparison of their performance at Wadi Tayyah Basin, Asir Region, Saudi Arabia. Landslides. 2015. https://doi.org/10.1007/s10346-015-0614-1
32. Hothorn T, Hornik K, Zeileis A. Unbiased Recursive Partitioning: A Conditional Inference Framework. Journal of Computational and Graphical Statistics. 2006; 15: 651–674. https://doi.org/10.1198/106186006X133933
33. Westfall PH, Young SS. Resampling-Based Multiple Testing: Examples and Methods for p-Value Adjustment. 1 edition. New York: Wiley-Interscience; 1993.
34. Wang S, Liu Y, Cairano-Gilfedder CD, Titmus S, Naim MM, Syntetos AA. Reliability Analysis for Automobile Engines: Conditional Inference Trees. Procedia CIRP. 2018; 72: 1392–1397. https://doi.org/10.1016/j.procir.2018.03.065
35. Cheng FW, Gao X, Bao L, Mitchell DC, Wood C, Sliwinski MJ, et al. Obesity as a risk factor for developing functional limitation among older adults: A conditional inference tree analysis. Obesity (Silver Spring). 2017; 25: 1263–1269. https://doi.org/10.1002/oby.21861 PMID: 28544480
36. Wu Z, Su X, Sheng H, Chen Y, Gao X, Bao L, et al. Conditional Inference Tree for Multiple Gene-Environment Interactions on Myocardial Infarction. Archives of Medical Research. 2017; 48: 546–552. https://doi.org/10.1016/j.arcmed.2017.12.001 PMID: 29258680

37. Porter KB, MacLean DA, Beaton KP, Upshall J, editors. New Brunswick permanent sample plot database (PSDB v1.0): user's guide and analysis. Fredericton, NB: Canadian Forest Service, Atlantic Forestry Centre, Natural Resources Canada; 2001.

38. SC. Ecological Land Classification, 2017. Ottawa: Statistics Canada; 2018. http://epe.lac-bac.gc.ca/100/201/301/weekly_acquisitions_list-ef/2018/18-09/publications.gc.ca/collections/collection_2018/statcan/12-607-x/12-607-x2018001-eng.pdf

39. Ecological Stratification Working Group (Canada). A National ecological framework for Canada. Ottawa: The Group; 1996.

40. Environment and Climate Change Canada. Canadian Climate Normals 1971–2000 Station Data—Climate—Environment and Climate Change Canada. 19 Jan 2011 [cited 30 Jul 2020]. https://climate.weather.gc.ca/climate_normals/results_e.html?stnID=5097&autofwd=1

41. NB Ecosystem Classification Working Group. Our Landscape Heritage. 2003 [cited 30 Jul 2020]. https://www2.gnb.ca/content/gnb/en/departments/erd/natural_resources/content/ForestsCrownLands/content/ProtectedNaturalAreas/OurLandscapeHeritage.html

42. Acker SA, Halpern CB, Harmon ME, Dyrness CT. Trends in bole biomass accumulation, net primary production and tree mortality in Pseudotsuga menziesii forests of contrasting age. Tree Physiol. 2002; 22: 213–217. https://doi.org/10.1093/treephys/22.2-3.213 PMID: 11830418

43. Coomes DA, Allen RB. Mortality and tree-size distributions in natural mixed-age forests. Journal of Ecology. 2007; 95: 27–40. https://doi.org/10.1111/j.1365-2745.2006.01179.x

44. Foster JR, D'Amato AW, Bradford JB. Looking for age-related growth decline in natural forests: unexpected biomass patterns from tree rings and simulated mortality. Oecologia. 2014; 175: 363–374. https://doi.org/10.1007/s00442-014-2881-2 PMID: 24442595

45. Gea-Izquierdo G, Férriz M, García-Garrido S, Aguín O, Elvira-Recuenco M, Hernandez-Escribano L, et al. Synergistic abiotic and biotic stressors explain widespread decline of Pinus pinaster in a mixed forest. Sci Total Environ. 2019; 685: 963–975. https://doi.org/10.1016/j.scitotenv.2019.05.378 PMID: 31247442

46. Reineke LH. Perfecting a Stand-Density Index for Even-Aged Forests. J Agricul Res. 1933; 46: 627–638.

47. Zhao D, Borders B, Wilson M. Individual-tree diameter growth and mortality models for bottomland mixed-species hardwood stands in the lower Mississippi alluvial valley. Forest Ecology and Management. 2004; 199: 307–322. https://doi.org/10.1016/j.foreco.2004.05.043

48. Yang Y, Titus SJ, Huang S. Modeling individual tree mortality for white spruce in Alberta. Ecological Modelling. 2003; 163: 209–222. https://doi.org/10.1016/S0304-3800(03)00008-5

49. Services of New Brunswick C. Service New Brunswick, Canada—SNB.CA. 10 Mar 2017 [cited 31 Jul 2020]. https://www2.snb.ca/content/snb/en.html

50. ESRI. Modeling solar radiation—Help | ArcGIS for Desktop. 2018 [cited 30 Jul 2020]. https://desktop.arcgis.com/en/Arcmap/10.3/Tools/Spatial-Analyst-Toolbox/Modeling-Solar-Radiation.Htm

51. Botkin DB. Forest Dynamics: An Ecological Model. Oxford; New York: Oxford University Press; 1993.

52. McKenney DW, Hutchinson MF, Papadopol P, Lawrence K, Pedlar J, Campbell K, et al. Customized Spatial Climate Models for North America. Bull Amer Meteor Soc. 2011; 92: 1611–1622. https://doi.org/10.1175/2011BAMS3132.1

53. Spearman C. The Proof and Measurement of Association between Two Things. The American Journal of Psychology. 1987; 100: 441. https://doi.org/10.2307/1422689 PMID: 3322052

54. Noh HG, Song MS, Park SH. An unbiased method for constructing multilabel classification trees. Computational Statistics & Data Analysis. 2004; 47: 149–164. https://doi.org/10.1016/j.csda.2003.10.009

55. Ma Z, Peng C, Li W, Zhu Q, Wang W, Song X, et al. Modeling Individual Tree Mortality Rates Using Marginal and Random Effects Regression Models. Natural Resource Modeling. 2013; 26: 131–153. https://doi.org/10.1111/j.1939-7445.2012.00124.x

56. Hawkes C. Woody plant mortality algorithms: description, problems and progress. Ecological Modelling. 2000; 126: 225–248. https://doi.org/10.1016/S0304-3800(00)00267-2

57. Lorimer C, Dahir SE, Nordheim EV. Tree mortality rates and longevity in mature and old-growth hemlock-hardwood forests. Journal of Ecology. 2001; 89: 960–971. https://doi.org/10.1046/j.0022-0477.2001.00619.x

58. Burns RM, Honkala BH. Silvics of North America: Conifers. Washington, DC: United States Department of Agriculture; 1990.

59. Burns RM, Honkala BH. Silvics of North America: Hardwoods. Washington, DC: United States Department of Agriculture; 1990.

60. Long ZT, Pendergast TH, Carson WP. The impact of deer on relationships between tree growth and mortality in an old-growth beech-maple forest. Forest Ecology and Management. 2007; 252: 230–238. https://doi.org/10.1016/j.foreco.2007.06.034

61. Chao K-J, Phillips OL, Gloor E, Monteagudo A, Torres-Lezama A, Martínez RV. Growth and wood density predict tree mortality in Amazon forests. Journal of Ecology. 2008; 96: 281–292. https://doi.org/10.1111/j.1365-2745.2007.01343.x

62. Stephenson NL, Das AJ, Condit R, Russo SE, Baker PJ, Beckman NG, et al. Rate of tree carbon accumulation increases continuously with tree size. Nature. 2014; 507: 90–93. https://doi.org/10.1038/nature12914 PMID: 24429523

63. Peet RK, Christensen NL. Competition and Tree Death. BioScience. 1987; 37: 586–595. https://doi.org/10.2307/1310669

64. Young DJN, Stevens JT, Earles JM, Moore J, Ellis A, Jirka AL, et al. Long-term climate and competition explain forest mortality patterns under extreme drought. Ecology Letters. 2017; 20: 78–86. https://doi.org/10.1111/ele.12711 PMID: 28000432

65. Peng C, Ma Z, Lei X, Zhu Q, Chen H, Wang W, et al. A drought-induced pervasive increase in tree mortality across Canada's boreal forests. Nature Climate Change. 2011; 1: 467–471. https://doi.org/10.1038/nclimate1293

66. McDowell NG, Allen CD. Darcy's law predicts widespread forest mortality under climate warming. Nature Climate Change. 2015; 5: 669–672. https://doi.org/10.1038/nclimate2641

67. Searls T, Zhu X, McKenney DW, Mazumder R, Steenberg J, Yan G, et al. Assessing the influence of climate on the growth rate of boreal tree species in northeastern Canada through long term permanent sample plot datasets. Can J For Res. 2020. https://doi.org/10.1139/cjfr-2020-0257

68. Boulanger Y, Gauthier S, Gray DR, Le Goff H, Lefort P, Morissette J. Fire regime zonation under current and future climate over eastern Canada. Ecological applications. 2013; 23: 904–923. https://doi.org/10.1890/12-0698.1 PMID: 23865239

69. Ishizuka M, Toyooka H, Osawa A, Kushima H, Kanazawa Y, Sato A. Secondary Succession Following Catastrophic Windthrow in a Boreal Forest in Hokkaido, Japan: The Timing of Tree Establishment. Journal of Sustainable Forestry. 1997; 6: 367–388. https://doi.org/10.1300/J091v06n03_08

70. MacLean DA, Andersen AR. Impact of a spruce budworm outbreak in balsam fir and subsequent stand development over a 40-year period. The Forestry Chronicle. 2008; 84: 60–69. https://doi.org/10.5558/tfc84060-1